Nanoscale Res Lett (2010) 5:130–137
DOI 10.1007/s11671-009-9454-z

NANO EXPRESS

Facile Synthesis of Monodisperse CdS Nanocrystals via Microreaction

Zhen Wan · Hongwei Yang · Weiling Luan · Shan-tung Tu · Xinggui Zhou

Received: 2 July 2009 / Accepted: 25 September 2009 / Published online: 13 October 2009

Abstract CdS-based nanocrystals (NCs) have attracted extensive interest due to their potential application as key luminescent materials for blue and white LEDs. In this research, the continuous synthesis of monodisperse CdS NCs was demonstrated utilizing a capillary microreactor. The enhanced heat and mass transfer in the microreactor was useful to reduce the reaction temperature and residence time to synthesize monodisperse CdS NCs. The superior stability of the microreactor and its continuous operation allowed the investigation of synthesis parameters with high efficiency. Reaction temperature was found to be a key parameter for balancing the reactivity of CdS precursors, while residence time was shown to be an important factor that governs the size and size distribution of the CdS NCs. Furthermore, variation of OA concentration was demonstrated to be a facile tuning mechanism for controlling the size of the CdS NCs. The variation of the volume percentage of OA from 10.5 to 51.2% and the variation of the residence time from 17 to 136 s facilitated the synthesis of monodisperse CdS NCs in the size range of 3.0–5.4 nm, and the NCs produced photoluminescent emissions in the range of 391–463 nm.

Keywords Microreaction · Quantum dots · CdS · Nanocrystals

Z. Wan · H. Yang · W. Luan (✉) · S. Tu
State Key Laboratory of Safety Science of Pressurized System, School of Mechanical and Power Engineering, East China University of Science and Technology, 200237 Shanghai, China
e-mail: luan@ecust.edu.cn

X. Zhou
State Key Laboratory of Chemical Engineering, East China University of Science and Technology, 200237 Shanghai, China

Introduction

The strong quantum confinement effect of colloidal semiconductor nanocrystals (NCs) has made these materials the subject of extensive research [1–5]. In the past decades, binary semiconductor NCs, identified as groups II–VI and III–V, have been studied intensively because of their size-dependent photoluminescence (PL) covering the spectrum range from ultraviolet to near infrared [6–10]. The importance of CdS NCs is manifested in their potential application as fluorescent materials with UV–blue PL emission [11–17]. The typical synthesis recipes for CdS NCs are based on a process that involves the injection of Cd-oleic acid (OA) into batch reactors. Nearly, monodispersed CdS NCs have been prepared using octadecene (ODE) as the non-coordinating solvent, and subsequent treatment of these NCs resulted in considerable improvement of PL efficiency. In these cases, the inefficient heat and mass transfer of batch reactors constrained the economical synthesis of CdS NCs. In order to overcome the energy barrier to form active monomers, a high reaction temperature (250–300°C) is generally required. Meanwhile, the temperature and concentration gradients involved in large reactors lead to poor quality and low process reproducibility. Furthermore, according to the International Commission on Illumination chromaticity diagram, the ideal wavelength for blue light is 460–480 nm. To achieve CdS NCs with blue PL emission, large CdS NCs with diameters greater than 5.2 nm are required. However, the preparation of these CdS NCs is limited by the high reaction temperature and long reaction time, where the advent of Ostwald ripening leads to wide size distributions.

The enhanced heat and mass transfer properties in the microenvironment could provide highly homogeneous

conditions for the chemical synthesis of NCs [18–24]. Compared with the batch reactor, a microreactor offers a controllable way to synthesize NCs continuously in a steady fashion [9, 20–23]. Meanwhile, the incorporation of novel channel structures and flow patterns facilitated the synthesis of monodisperse NCs in an accelerated manner. However, the limited research conducted to date on the microfluidic synthesis of CdS NCs has been based on aqueous processes, and the resulting NCs generally had wide size distributions and deep-trap luminescence that overwhelmed the visible range [19, 25–27]. Droplet microfluidics has been demonstrated as a powerful tool for achieving efficient mixing, while realizing highly homogeneous environment for the synthesis of monodisperse CdS NCs [27], but its low throughput limits its use to commercial-scale synthesis.

In this study, a capillary microreactor was used for the accelerated synthesis of monodisperse CdS NCs. In order to obtain high-quality samples, systematic investigations of temperature and residence time requirements were conducted. Also, a quantitative investigation of the influence of OA on size distribution and growth kinetics was conducted to achieve the size-controlled synthesis of CdS NCs. The influence of OA on the reaction kinetics was evidenced by the collected absorption spectra. In addition, the high quality of the resulting CdS NCs was confirmed by the PL spectra, powder X-ray diffraction (XRD), and high-resolution transmission electron microscopy (HRTEM).

Experimental

Raw Materials

Cadmium oxide (CdO, SCR, 99.9%), sulfur (S, SCR, 99.5%), 1-octadecene (ODE, Fisher, 90%), oleic acid (OA, SCR, 90%), and analytic grade acetone and chloroform (SCR) were used directly without further processing.

Synthesis of CdS NCs

CdS NCs were prepared using a recipe similar to the one previously reported by Yu et al. [17]. Typically, 1 mmol CdO, 4.5 mmol OA, and ODE (5 ml in total) were mixed together and heated to 150°C under a nitrogen atmosphere for 1 h with vigorous stirring to prepare a clear, yellow, cadmium-precursor solution. Meanwhile, a stock solution of sulfur was prepared by dissolving 1 mmol S powder in ODE (5 ml in total) at 150°C with magnetic stirring for 1.5 h.

The microfluidic reactor included a precursor delivery system, a convective micromixer (50 μl), and a length of polytetrafluoroethylene (PTFE) capillary (ID = 462 μm, length = 50 cm), as shown in Fig. 1. Equal volume solutions of Cd and S precursors were delivered by a syringe pump (Harvard 22, USA) at the same flow rate, and the precursors were combined and mixed in a magnetic micromixer. Then, the mixture of precursors was placed in a heated PTFE capillary where nucleation and growth of the NCs occurred at a constant reaction temperature of 220°C. A thermally stable oil bath was used as a heat source, and the flow rate of the precursors was set at 4.47 ml h^{-1} to achieve a residence time of 68 s. During the optimization process for OA concentration, various amounts of OA were replaced by ODE, while maintaining a constant volume of solution. The samples were collected and diluted with chloroform for further characterization of their spectra. The entire process was performed in air. Details of the microreaction system were described previously [9].

Apparatus

UV–vis absorption spectra were recorded on a Cary 50 UV–vis spectrometer (Varian, USA) at room temperature. PL spectra were measured at room temperature with a Cary Eclipse spectrofluorometer (Varian, USA) for colloidal solutions with an optical density of less than 0.2 at an excitation wavelength of 330 nm. Quantum yields (QY) of

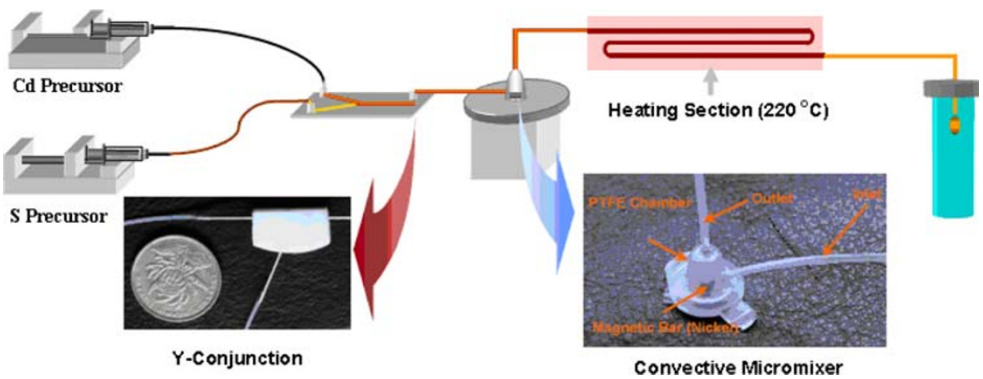

Fig. 1 Schematic representation of the capillary microfluidic reactor

PL was obtained by comparing the integrated PL intensities of the NCs with the organic dye (Rhodamine 6G) [11]. To obtain samples for TEM and XRD characterization, the formed CdS NCs were precipitated by adding acetone into their chloroform solution; the NCs were isolated and purified by repeated centrifugation and decantation. XRD patterns were obtained using a D/max-2550 diffraction meter (Rigaku, Japan) with a Cu anode. During the preparation of samples for XRD analysis, an Si wafer was used as a support to minimize background noise. The morphologies and dimensions of the as-formed NCs were observed by a JEM-2100F HRTEM (JEOL, Japan). The samples for HRTEM observations were obtained by dipping a carbon–copper grid in a dilute, chloroform-dispersed solution of NCs.

Results and Discussion

In batch reactions, the long response time for temperature stabilization and the vibration at reaction conditions make it difficult to achieve precise control of the sizes of CdS NCs. On the contrary, microreaction provides a reproducible tool for synthesizing NCs in a highly controllable manner. Furthermore, the enhanced heat and mass transfer in a microreactor greatly improves the concentrations of reactive monomers, resulting in reductions in the reaction temperature and residence time required to form high-quality NCs.

In order to achieve a balance between process stability and the reactivity of precursors, the reaction temperature and residence time were systematically investigated.

During the synthesis of NCs, the reaction temperature is an important parameter that determines both the ligand and reaction kinetics. Low temperatures are insufficient for overcoming the energy barrier for highly reactive monomers, while high temperatures that exceed a threshold lead to the early advent of Ostwald ripening. In this study, the reaction temperature was adjusted from 180 to 260°C at a constant residence time of 68 s. Figure 2 shows the absorption and PL spectra as well as the kinetics data of CdS NCs prepared at various reaction temperatures. Generally, the sharp band-edge absorbance with a half width at half maximum (HWHM) value of 12 nm and several higher transitions are clearly resolved for CdS NCs that were synthesized at temperatures above 200°C. Whereas, due to the weak reactivity, the magic-size cluster was observed at 180°C, indicated by the appearance of an absorption peak with a wavelength of almost 320 nm. In addition, pure band-gap emissions with very narrow full width at half maximum (FWHM ~ 17 nm) were observed at 220°C. The earlier mentioned results clearly point to a narrow size distribution and well-passivated surfaces of the CdS NCs. When the temperature was increased from 180 to 240°C, a 44-nm redshift in the PL peak was observed, indicating that the growth rate of the NCs improved at the higher temperatures. However, impurities in the technical grade ODE resulted in the evolution of gas at high reaction temperatures above 240°C. The presence of the gas decreased the residence time and induced the blueshift of the PL peak.

FWHM of PL is an indirect measure for the size distribution of NCs. In Fig. 2c, it can be seen that FWHM of the NCs tended to decrease when the temperature was changed from 180 to 220°C. Further increases in the temperature led to wider FWHM values. During the diffusion-controlled synthesis of spherical NCs, the burst of

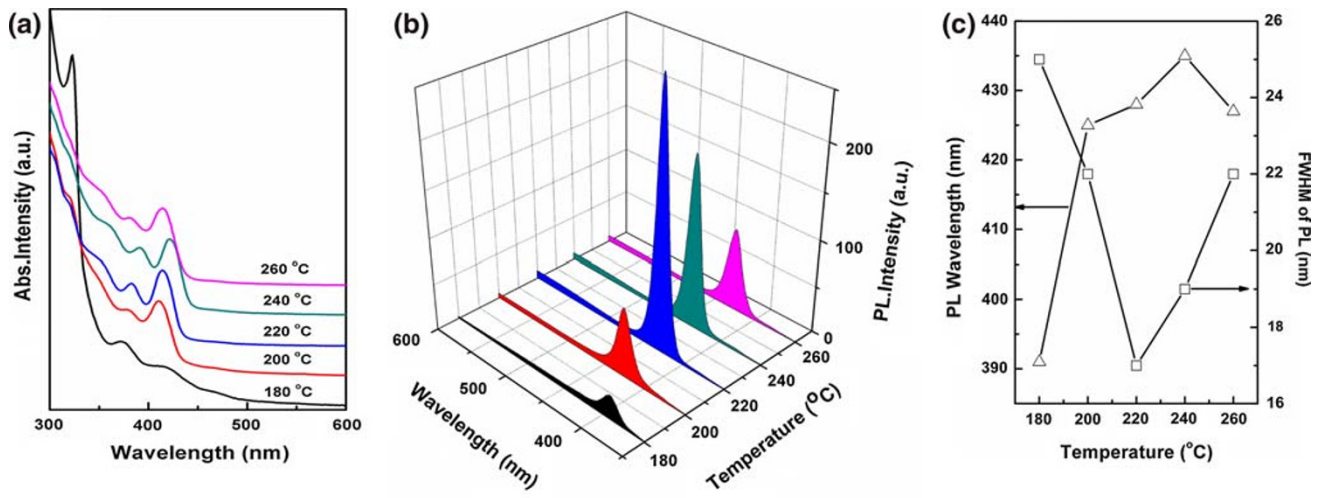

Fig. 2 **a** Absorption, **b** PL spectra, and **c** relative kinetics of CdS NCs prepared at various temperatures at a constant residence time of 68 s (OA: 15. 6 vol %)

nucleation that separated from the growth is the prerequisite for achieving monodisperse products [28]. Temperatures below 180°C cannot overcome the energy barrier to form the reactive monomer species, which restricted the burst of nucleation. The nucleation in the whole reaction phase led to poor size distribution. With the increase in reaction temperature from 180 to 220°C, the continuously increased reactivity of the monomer allowed the burst of nucleation, leading to gradual narrowing of the size distribution. The narrowest FWHM was observed at 220°C, indicating a balance of nucleation and growth at this temperature, which is a threshold after which the widened FWHM was induced by further increases in temperature.

The underlying kinetics for the growth of NCs played an important role in the observed FWHM in Fig. 2c. For the diffusion-controlled growth of spherical NCs, the size(r)-dependent growth rate (dr/dt) of NCs has a maximum at a critical radius r_{cr}. When $r > r_{cr}$, the smaller NCs grow faster than the larger ones, resulting in a narrower size distribution. When $r < r_{cr}$, the smaller NCs grow slower than the larger ones or even dissolve in the solution (Ostwald ripening), which led to a broad size distribution of the final products. In our experiment, temperatures above 220°C resulted in the rapid depletion of monomers, and the low concentration of monomers led to a larger critical size. As a result, large NCs grew from the monomers formed by the dissolution of small NCs, and broad FWHM was observed with the increase in temperature.

The microfluidic reaction facilitated the process of optimization using a minimal amount of precursors. In this study, the optimization process for the reaction temperature was achieved within an hour, while consuming less than 1 ml of the precursors. Furthermore, the enhanced heat and mass transfer in the microreactor resulted in a reduction in the temperature required to achieve the synthesis of high-quality NCs. In our work, monodisperse CdS NCs were synthesized at a fairly low temperature of 220°C, which is among the lowest values reported based on other studies using similar recipes [17].

The evaluation of residence time was achieved by changing the flow rate from 17.8 to 2.22 ml h^{-1}. Figure 3 compares the absorption and PL spectra, as well as relative kinetic data, of the samples prepared at residence times ranging from 17 to 136 s at a constant reaction temperature of 220°C. The sharp band-edge absorbance and three higher transitions, as well as band-gap emissions, can be clearly observed, displaying the high quality of the as-formed NCs. As shown in Fig. 3b, the increased residence time induced a 30-nm redshift of the PL peak, elucidating the growth of NCs. Concerning the FWHM of PL, the optimal residence time was observed to be 68 s when a narrow FWHM of only 17 nm was observed. With the increase in residence time from 17 to 68 s, the FWHM of PL continuously decreased from 20 to 17 nm, indicating the focusing of the size distribution in this phase, whereas increasing the residence time beyond 68 s resulted in increased FWHM values. In the early reaction stage, the high monomer concentration led to a small r_{cr}, which is smaller than the normal size of the NCs presented in the solution. In this phase, small NCs exhibited a more rapid growth rate than large NCs, and the size distribution of the NCs continuously focused. Meanwhile, the velocity of the CdS NCs had a parabolic profile inside the capillary, while induced residence time distribution (RTD) for CdS NCs. Numerical simulation and experimental results demonstrated that the RTD effect becomes trivial at low flow rates (corresponding to long residence time in this study). As a result, the above two effects justified the narrowed FWHM observed in the early reaction stage. The prolonged growth time resulted in low monomer concentration, which led to

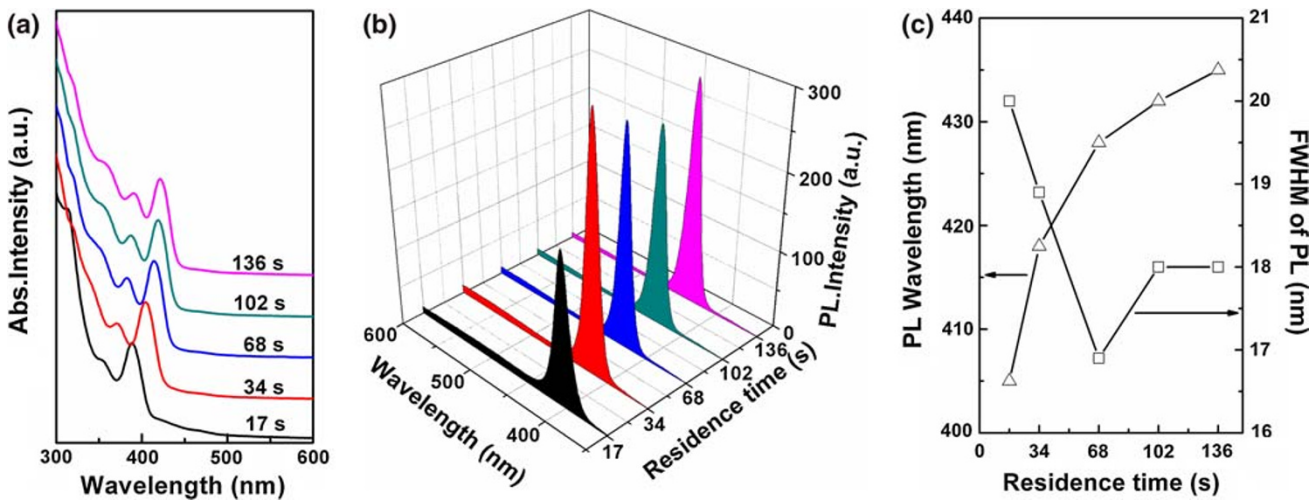

Fig. 3 **a** Absorption, **b** PL spectra, and **c** Relative kinetics of CdS NCs synthesized at different residence times (with a constant reaction temperature of 220°C, OA: 15. 6 vol %)

large r_{cr}, and the size of some CdS NCs fell below r_{cr} while the advent of Ostwald ripening led to increased FWHM of PL for CdS NCs.

In this paper, OA was utilized as the ligand for the formation of cationic precursors and passivation of the NCs, while ODE was chosen as the non-coordinating solvent. Size and size distribution can be simply tuned by varying the concentration of ligands in the solution. Therefore, the influence of OA was systematically investigated. The temporal evolutions of UV–vis spectra at various residence times were recorded at different volume percentages of OA, as shown in Fig. 4. The discrete reactions were performed under identical conditions, except for the concentration of OA in the reaction mixture. During the variation of volume ratio for OA over a wide range (10.5–51.2 vol %) and the variation of residence time from 17 to 136 s, monodisperse CdS NCs were obtained in different size ranges, which were clearly shown by the observation of a sharp absorption peak (HWHM ~ 12 nm) and up to three excitonic transition states. With the increase in residence time and the variety of ligand concentrations, a 64-nm shift of absorption peaks (from 389 to 453 nm) was obtained.

The wavelength of the first excitonic absorption peak and the corresponding absorption intensity, as well as HWHM, was utilized to calculate the mean particle diameter and particle number of the obtained CdS NCs, using the empirical fitting function reported by Yu [29]. In Fig. 5, the data obtained appear to show a significant influence of OA on the mean size and size distribution of CdS NCs. At the same residence time, a high volume percentage of OA resulted in large particle sizes and low particle concentration. Taking the residence time of 68 s as an example, tuning the volume percentage of OA from 10.5 to 51.2% led to a significant increase in the mean diameter of the NCs from 3.8 to 5.3 nm, accompanied by dramatic decrease in particle concentration from 2.20×10^{20}/l to 0.20×10^{20}/l. Since OA restrains the formation of nuclei during the nucleation process, the low particle concentration was observed at high OA concentrations. Furthermore, the analysis conducted by Peng et al. [17] indicated that the depletion rate of monomers was basically constant after the primal stage of the reactions, even though different initial OA concentrations were used. As a result, for CdS NCs that were prepared by utilizing high OA concentrations, less nuclei were formed while the depletion rate of the Cd-OA monomers kept the same, compared with low OA concentrations. The combination of the above two factors led to a rapid growth rate of NCs, resulting in large particle sizes and low particle concentrations. At the same time, the

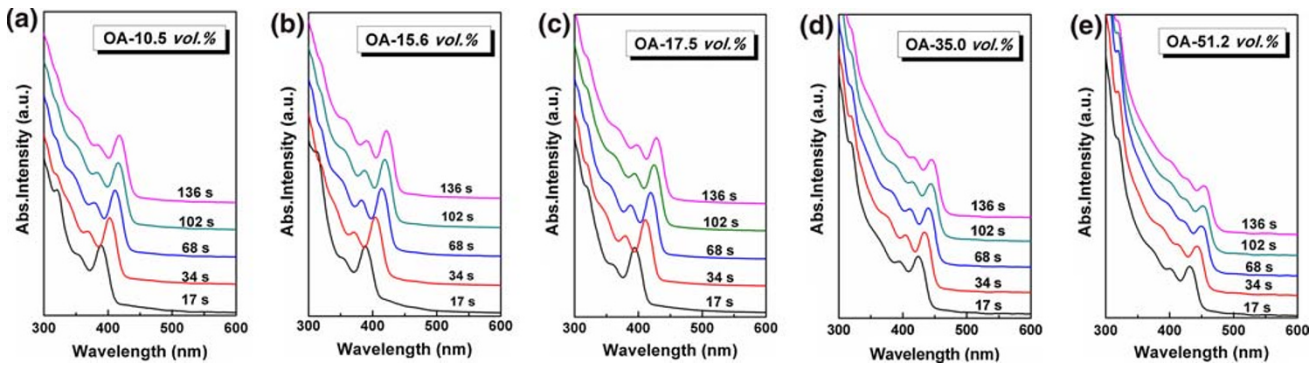

Fig. 4 Absorption spectra of the samples monitored during the evolution of residence time and OA volume (OA only in Cd side, $T = 220$°C)

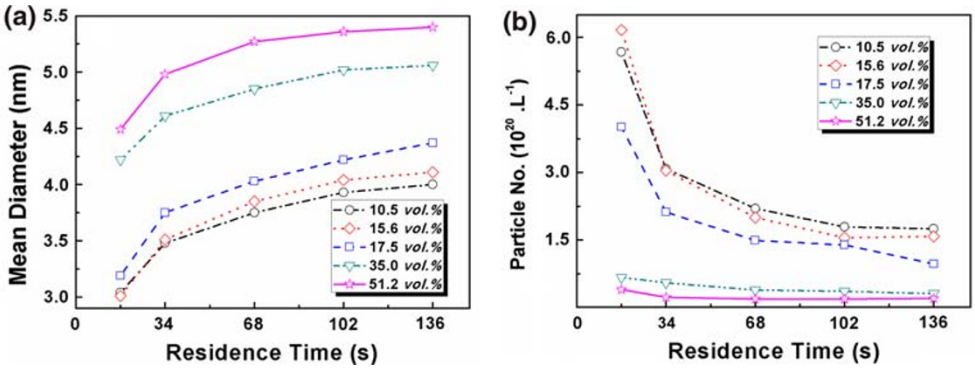

Fig. 5 **a** Mean diameter and **b** Particle concentration of the CdS samples prepared during the evolution of residence time and volume percentage of OA (OA only in Cd side, $T = 220$°C)

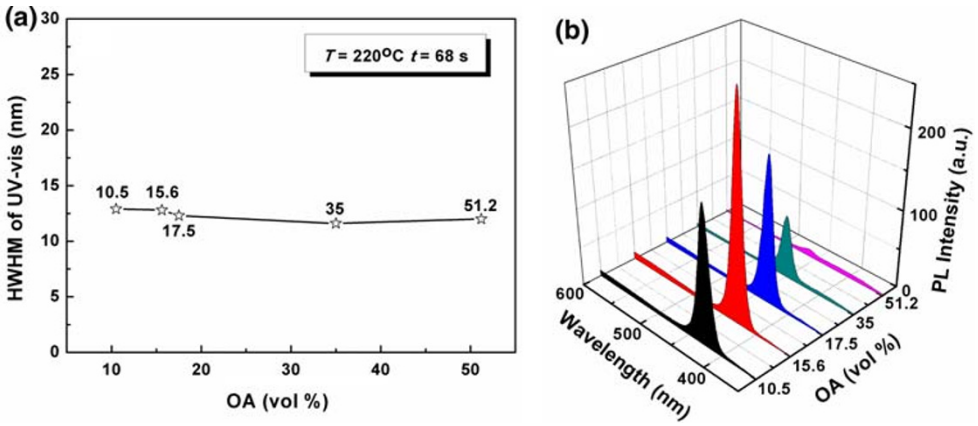

Fig. 6 **a** HWHM of UV–vis and **b** PL intensity of CdS samples prepared at various volume percentage of OA ($T = 220°C$, $t = 68$ s)

rapid growth negated the annealing process and led to higher concentrations of surface defects, which led to weak PL intensity.

In batch reactions, CdS NCs prepared using high OA concentrations generally demonstrated wide size distribution. However, monodisperse (HWHM ~ 11 nm) CdS NCs can be obtained with a high volume ratio of OA of 51.2%, and the size of the CdS NCs were in the range of 4.5–5.3 nm in the microreaction. The efficient mixing and heat transfer, as well as uniform reaction conditions, achieved by the microreactor contributed to the formation of the high-quality products. In addition, the narrow diffusion length along the radius of the microchannels created homogeneous reaction conditions for the uniform growth of CdS NCs, even at rapid growth rate that was induced by high OA concentrations.

The HWHM and PL spectra of the CdS NCs prepared using various volume percentages of OA are shown in Fig. 6. To create the same baseline for the comparison of PL intensity, the absorbance of the samples at the excitation wavelength was adjusted to be the same. Figure 6a shows that a narrower HWHM of approximately 13 nm can be obtained for different OA content, indicating the narrow size distribution of the resulting NCs. However, with the increase in the volume ratio of OA, a significant improvement of PL intensity was observed and reached the highest value when applying volume ratio of OA as 15.6 vol % (Fig. 6b), while further increases in the volume ratio resulted in decreased PL intensity. For CdS NCs prepared using a volume ratio of 51.2%, the deep-trap emission made the samples demonstrate red color under an UV lamp. The PL efficiency of the NCs was mainly governed by the surface state of the NCs. The slow growth rate induced by the low OA concentration and the optimal ligand capping at 15.6 vol % resulted in the best PL efficiency, while the improved growth rate that accompanied the increase in OA concentration resulted in increased defects on the surface of NCs, which justified the low PL intensity under high OA concentration above 35 vol %. For all the obtained samples, the QY were laid between 2.0 and 14.5%. The QY could be improved by the surface capping with ZnS shell [21], and this research is under active investigation in our group.

Just by varying the volume ratio of OA and residence time, various sizes of high-quality CdS NCs ranging from 3.0 to 5.4 nm were obtained at the fairly low reaction temperature of 220°C (Fig. 7), corresponding to PL peak wavelengths of 391–463 nm. The band-gap emission was observed when the particle size was smaller than 5 nm.

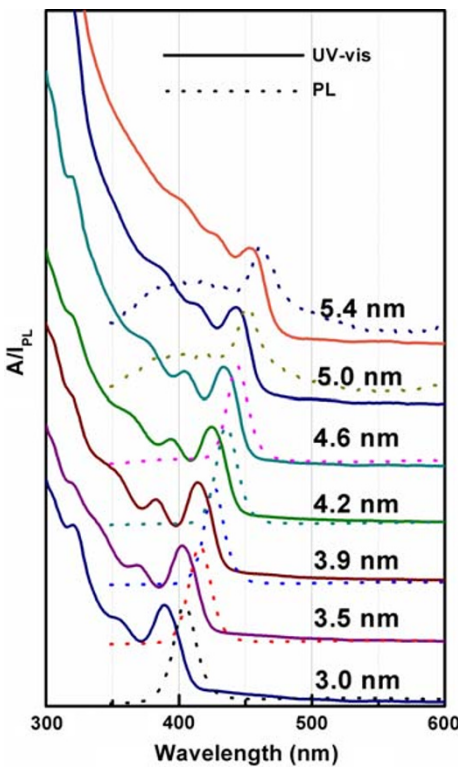

Fig. 7 UV–vis absorption and PL spectra of the as-prepared CdS NCs with various mean sizes. (*A* absorption intensity, I_{PL} = PL intensity)

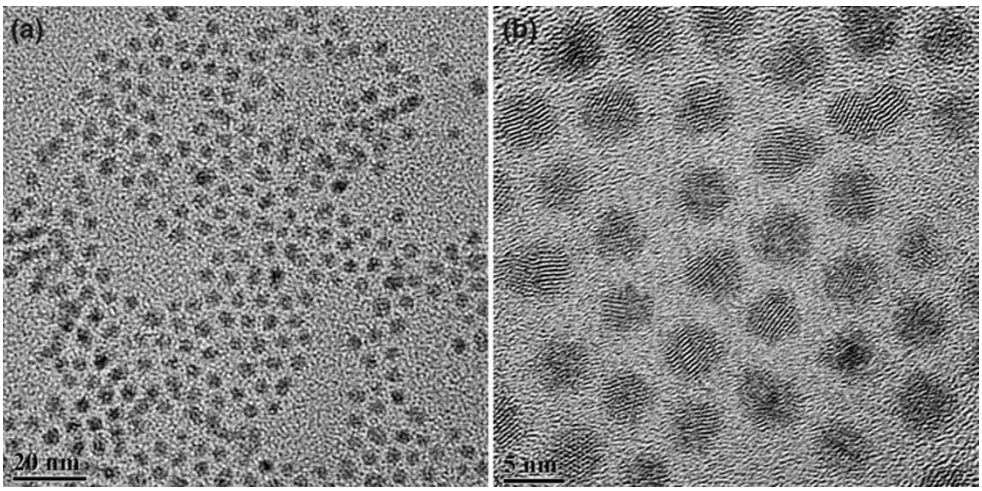

Fig. 8 **a** TEM and **b** HRTEM images of CdS NCs (band-gap absorption of 449 nm with an HWHM value of 11 nm) synthesized in open air via microreaction

Therefore, due to the high quality of the as-prepared CdS NCs, ZnS–capped CdS core–shell structure NCs with excellent blue luminescence efficiency, color purity, and a narrow size distribution can easily be obtained.

Figure 8 shows TEM and HRTEM images of CdS NCs, which clearly display the narrow size distribution and fairly spherical morphology of the CdS NCs with an average diameter of 5.2 nm. Statistical calculations for the 50 dots in a selected regime produced a 6% standard deviation of the average diameter. Furthermore, the distinguishable lattice plane revealed the high crystallinity of the dots. Figure 9 shows the XRD spectra of 5.2-nm CdS NCs, which exhibited a typical pattern of the zinc-blende structure with three distinct features. The first diffraction peak at $2\theta = 27°$ corresponded to the (111) reflection, and the other two features, which appeared at $2\theta = 44°$ and 52°, corresponded to the (220) and (311) reflections, respectively.

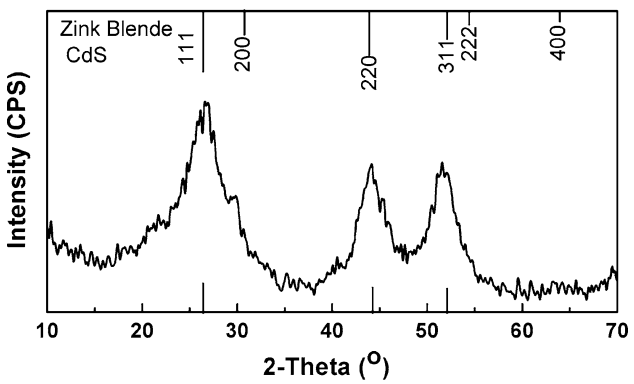

Fig. 9 XRD pattern of 5.2-nm CdS NCs synthesized at 68 s (OA: 51.2 vol %)

Conclusions

In conclusion, a capillary microreactor was used for the continuous synthesis of CdS NCs, and the influences of reaction temperature and residence time were investigated systematically to obtain the optimal synthesis parameters. The enhanced mass and heat transfer involved in microchannels facilitated the rapid synthesis of high-quality CdS NCs at the low reaction temperature of 220°C. The combined effect of RTD and Ostwald ripening resulted in the optimal residence time as 68 s. The continuous operation and low sample consumption involved in microreaction allowed an accelerated study of the kinetics involved. Variations of OA concentration and residence time were demonstrated as an effective way to control the size of CdS NCs produced. With an increase in residence time from 17 to 136 s and an increase in the volume percentage of OA from 10.5 to 51.2%, CdS NCs in the size range from 3.0 to 5.4 nm were obtained, with corresponding PL peak wavelength from 391 to 463 nm. With the careful selection of reaction parameters, a moderate QY as 14.5% was obtained. Furthermore, excellent size distributions were obtained over a wide range of OA concentrations, and narrow HWHM absorption peaks (from 11.6 to 14.0 nm) were maintained during the entire process.

Acknowledgments Authors appreciated the financial supports from the NSFC (50772036), The Focus of Scientific and Technological Research Projects (109063) and the State Key Laboratory of Chemical Engineering at ECUST (SKL-ChE-08C09).

References

1. M. Bruchez Jr., M. Moronne, P. Gin et al., Science **281**, 2013 (1998)

2. X. Michalet, F.F. Pinaud, L.A. Bentolila et al., Science **307**, 538 (2005)
3. Y.D. Yin, A.P. Alivisatos, Nature **437**, 664 (2005)
4. S. Coe, W.K. Woo, M.G. Bawendi et al., Nature **420**, 800 (2002)
5. K.T. Thurn, E.M.B. Brown, A. Wu, Nanoscale Res. Lett. **2**, 430 (2007)
6. E. Stephen, M.G. Bawendi, Acc. Chem. Res. **32**, 389 (1999)
7. S. Sapra, L. Rogach, J. Feldmann, J. Mater. Chem. **33**, 3391 (2006)
8. L.S. Li, N. Pradhan, Y.J. Wang et al., Nano Lett. **4**, 2261 (2004)
9. W.L. Luan, H.W. Yang, S.T. Tu et al., Nanotechnology **18**, 175603 (2007)
10. L.H. Qu, X.G. Peng, J. Am. Chem. Soc. **124**, 2049 (2002)
11. M. Protière, P. Reiss, Nanoscale Res. Lett. **1**, 62 (2006)
12. Z.A. Peng, X.G. Peng, J. Am. Chem. Soc. **123**, 183 (2001)
13. Y.C. Cao, J.H. Wang, J. Am. Chem. Soc. **126**, 14336 (2004)
14. J.S. Steckel, J.P. Zimmer, S.C. Sullivan et al., Angew. Chem. Int. Ed. **43**, 2154 (2004)
15. C.B. Murray, D.J. Norris, M.G. Bawendi, J. Am. Chem. Soc. **115**, 8706 (1993)
16. J. Joo, H.B. Na, T. Yu et al., J. Am. Chem. Soc. **125**, 11100 (2003)
17. W.W. Yu, X.G. Peng, Angew. Chem. Int. Ed. **41**, 2368 (2002)
18. M. Boutonnet, J. Kizling, P. Stenius et al., Colloids Surf. **5**, 209 (1982)
19. J.B. Edel, R. Fortt, J.C. deMello et al., Chem. Commun. **10**, 1136 (2002)
20. H.W. Yang, W.L. Luan, S.T. Tu et al., Lab Chip **8**, 451 (2008)
21. W.L. Luan, H.W. Yang, N.N. Fan et al., Nanoscale Res. Lett. **3**, 134 (2008)
22. H. Nakamura, Y. Yamaguchi, M. Miyazaki et al., Chem. Commun. **23**, 2844 (2002)
23. H.Z. Wang, X.Y. Li, M. Uehara et al., Chem. Commun. **1**, 48 (2004)
24. X.X. Zhu, Q.H. Zhang, Y.G. Li et al., J. Mater. Chem. **18**, 5060 (2008)
25. E.M. Chan, R.A. Mathies, A.P. Alivisatos, Nano Lett. **3**, 199 (2003)
26. E.M. Chan, A.P. Alivisatos, R.A. Mathies, J. Am. Chem. Soc. **127**, 13854 (2005)
27. I. Shestopalov, J.D. Tice, R.F. Ismagilov, Lab Chip **4**, 316 (2004)
28. X.G. Peng, J. Wickham, A.P. Alivisatos, J. Am. Chem. Soc. **120**, 5343 (1998)
29. W.W. Yu, L.H. Qu, W.Z. Guo et al., Chem. Mater. **15**, 2854 (2003)